

Journal of
Mechanics of
Materials and Structures

**ANTIPLANE DEFORMATION OF ORTHOTROPIC STRIPS WITH
MULTIPLE DEFECTS**

Reza Teymori Faal, Shahriar J. Fariborz and Hamid Reza Daghyani

Volume 1, N° 7

September 2006

 mathematical sciences publishers

ANTIPLANE DEFORMATION OF ORTHOTROPIC STRIPS WITH MULTIPLE DEFECTS

REZA TEYMORI FAAL, SHAHRIAR J. FARIBORZ AND HAMID REZA DAGHYANI

Stress analysis is carried out in an orthotropic strip containing a Volterra-type screw dislocation. The distributed dislocation technique is employed to obtain integral equations for a strip weakened by cracks and cavities under antiplane traction. These equations are of Cauchy singular kind, which are solved numerically by generalizing a numerical method available in the literature. Several examples are solved to demonstrate the validity and applicability of the procedure.

1. Introduction

In composite materials, defects in the form of cracks and cavities generate regions of high stress gradient. These regions are the primary locus of failure in structures, even under moderate applied load. Therefore, stress analysis in the vicinity of defects is imperative as the first stage of the design process.

Stress analysis in a strip with cracks under antiplane deformation has been investigated frequently. Here, we review some recent pertinent articles. Zhou et al. [1998] showed that in the vicinity of two collinear cracks perpendicular to the edges of an isotropic strip, the cracks were symmetrical with respect to the centerline of the strip and subjected to antiplane traction. Li [2003] obtained a closed-form solution for orthotropic strips. Stress analysis in an isotropic strip weakened by two collinear cracks situated on the centerline under antiplane shear was carried out by [Zhou and Ma 1999]. In the above articles, the application of boundary conditions resulted in a set of integral equations which are solved by the Schmidt's method. Wu and Dzenis [2002] obtained closed-form solutions for mode III stress intensity factors for an interfacial edge crack between two bonded semi-infinite dissimilar elastic strips. Li [2005] considered an interfacial crack between two bonded dissimilar semi-infinite orthotropic strips where the crack surface was under antiplane traction. Closed form stress intensity factors were obtained for a strip with either clamped or traction-free boundaries.

In this study, we perform stress analysis in an orthotropic strip weakened by cracks and cavities under antiplane deformation. We obtain the solution of Volterra-type screw dislocation by means of Fourier transformation, and use the solution to derive integral equations for cracks. Cavities are considered as closed curved cracks without singularity. The integral equations are solved numerically for the dislocation density function by generalizing the method developed by [Erdogan et al. 1973] to take into account cavities, embedded cracks, and edge cracks. Finally, we obtain the stress intensity factor for cracks, and the hoop stress for cavities for several examples.

We regret to inform that Hamid Reza Daghyani passed away in 2006.

Keywords: antiplane deformation, orthotropic strip, multiple defects, Cauchy-type singularity.

2. Strip with screw dislocation

The distributed dislocation technique is an efficient means of treating multiple curved cracks with smooth geometries. However, determining stress fields due to a single dislocation in the region has been a major obstacle to the utilization of this method. We now take up this task for an orthotropic strip containing a screw dislocation. We consider an orthotropic elastic strip with finite thickness h in the y -direction and extended infinitely in the x -direction. The x -axis is situated at the distance h_1 below the upper edge of the strip. The only nonzero displacement component under antiplane deformation is the out of plane component $w(x, y)$. Consequently, the constitutive relationships are

$$\sigma_{zy} = G_{zy} \frac{\partial w}{\partial y}, \quad (1)$$

$$\sigma_{zx} = G_{zx} \frac{\partial w}{\partial x}. \quad (2)$$

In the above equalities, G_{zx} and G_{zy} are the orthotropic shear moduli of elasticity of material. The equilibrium equations $\sigma_{ij,j} = 0$, in view of Equations (1)–(2), reduce to

$$G_{zx} \frac{\partial^2 w}{\partial x^2} + G_{zy} \frac{\partial^2 w}{\partial y^2} = 0. \quad (3)$$

The traction-free condition on the strip edges implies that

$$\sigma_{zy}(x, h_1) = 0, \quad \sigma_{zy}(x, h_1 - h) = 0. \quad (4)$$

A Volterra-type screw dislocation with Burgers vector δ is situated at the origin of coordinates with the dislocation line $x = 0, y > 0$. The conditions representing the dislocation are

$$\lim_{|x| \rightarrow \infty} w = 0, \quad (5)$$

$$w(0^+, y) - w(0^-, y) = \delta H(y), \quad (6)$$

where $H(y)$ is the Heaviside step function. The conditions of continuity and self-equilibrium of stress in the strip containing dislocation imply that

$$w(x, 0^-) = w(x, 0^+), \quad \sigma_{zy}(x, 0^-) = \sigma_{zy}(x, 0^+). \quad (7)$$

Since the problem is symmetric with respect to the y -axis, we may consider only the region $x > 0$. Equation (3) is solved by Fourier sine transformation, which for a sufficiently regular function $f(x)$ is defined as

$$F(\lambda) = \int_0^\infty f(x) \sin \lambda x \, dx. \quad (8)$$

The inversion of the Fourier sine transform yields

$$f(x) = \frac{2}{\pi} \int_0^\infty F(\lambda) \sin \lambda x \, d\lambda. \quad (9)$$

The application of Equation (8) to Equation (3) with the aid of Equation (5) leads to a second order ordinary differential equation, in each region $0 \leq y \leq h_1$ and $h_1 - h \leq y \leq 0$. The solution satisfying

Equation (6) is readily known, namely

$$W(\lambda, y) = \begin{cases} a_1 e^{\lambda G y} + b_1 e^{-\lambda G y} + \frac{\delta}{2\lambda}, & 0 \leq y \leq h_1, \\ a_2 e^{\lambda G y} + b_2 e^{-\lambda G y}, & h_1 - h \leq y \leq 0, \end{cases} \tag{10}$$

where $G = \sqrt{G_{zx}/G_{zy}}$. The application of conditions (4) and (7) to Equation (10) results in

$$a_1 = \frac{\delta e^{-2\lambda G h_1} (e^{2\lambda G h} - e^{2\lambda G h_1})}{4\lambda(1 - e^{2\lambda G h})}, \quad b_1 = \frac{\delta (e^{2\lambda G h} - e^{2\lambda G h_1})}{4\lambda(1 - e^{2\lambda G h})}, \tag{11}$$

$$a_2 = \frac{\delta e^{2\lambda G h} (e^{-2\lambda G h_1} - 1)}{4\lambda(1 - e^{2\lambda G h})}, \quad b_2 = \frac{\delta (1 - e^{2\lambda G h_1})}{4\lambda(1 - e^{2\lambda G h})}. \tag{12}$$

The displacement field in view of Equations (9)–(12) becomes

$$w(x, y) = \frac{\delta}{2\pi} \int_0^\infty \left(\frac{(e^{2\lambda G h} - e^{2\lambda G h_1})(e^{\lambda G(y-2h_1)} + e^{-\lambda G y})}{\lambda(1 - e^{2\lambda G h})} + \frac{2}{\lambda} \right) \sin \lambda x \, d\lambda, \quad 0 \leq y \leq h_1, \tag{13}$$

$$w(x, y) = \frac{\delta}{2\pi} \int_0^\infty \left(\frac{(e^{-2\lambda G h_1} - 1)(e^{\lambda G(y+2h)} + e^{-\lambda G(y-2h_1)})}{\lambda(1 - e^{2\lambda G h})} \right) \sin \lambda x \, d\lambda, \quad h_1 - h \leq y \leq 0. \tag{14}$$

Note that the rigid body motion of strip, that is, the unboundedness of the integrand in Equation (13) as $\lambda \rightarrow \infty$, may cause difficulties in carrying out the above integrations. Consequently, it is expedient to obtain the displacement field from the stress components instead. Substituting Equations (13)–(14) into

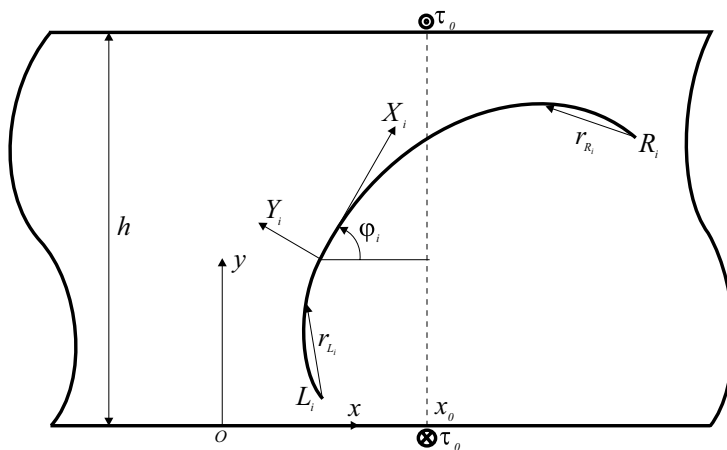


Figure 1. Schematic view of the strip with a curved crack.

Equations (1)–(2) yields

$$\sigma_{zy}(x, y) = \frac{\delta G G_{zy}}{2\pi} \int_0^\infty \frac{(e^{2\lambda Gh} - e^{2\lambda Gh_1})(e^{\lambda G(y-2h_1)} - e^{-\lambda Gy})}{1 - e^{2\lambda Gh}} \sin \lambda x \, d\lambda, \quad 0 \leq y \leq h_1, \quad (15)$$

$$\sigma_{zx}(x, y) = \frac{\delta G_{zx}}{2\pi} \int_0^\infty \frac{(e^{2\lambda Gh} - e^{2\lambda Gh_1})(e^{\lambda G(y-2h_1)} + e^{-\lambda Gy})}{1 - e^{2\lambda Gh}} \cos \lambda x \, d\lambda, \quad 0 \leq y \leq h_1, \quad (16)$$

$$\sigma_{zy}(x, y) = \frac{\delta G G_{zy}}{2\pi} \int_0^\infty \frac{(e^{-2\lambda Gh_1} - 1)(e^{\lambda G(y+2h)} - e^{-\lambda G(y-2h_1)})}{1 - e^{2\lambda Gh}} \sin \lambda x \, d\lambda, \quad h_1 - h \leq y \leq 0, \quad (17)$$

$$\sigma_{zx}(x, y) = \frac{\delta G_{zx}}{2\pi} \int_0^\infty \frac{(e^{-2\lambda Gh_1} - 1)(e^{\lambda G(y+2h)} + e^{-\lambda G(y-2h_1)})}{1 - e^{2\lambda Gh}} \cos \lambda x \, d\lambda, \quad h_1 - h \leq y \leq 0. \quad (18)$$

The integrals in Equations (15)–(18) can be evaluated employing contour integration and the residue theorem. The stress components are obtained in series form which are summed, leading, in the whole strip region, to

$$\sigma_{zy}(x, y) = \frac{\delta G_{zy} \sinh \kappa x}{4h} \left(\frac{1}{\cosh \kappa x - \cos \kappa Gy} - \frac{1}{\cosh \kappa x - \cos \kappa G(y - 2h_1)} \right), \quad (19)$$

$$\sigma_{zx}(x, y) = \frac{\delta G G_{zy}}{4h} \left(\frac{\sin \kappa(y - 2h_1)}{\cosh \kappa x - \cos \kappa G(y - 2h_1)} - \frac{\sin \kappa y}{\cosh \kappa x - \cos \kappa Gy} \right), \quad (20)$$

where $\kappa = \pi/Gh$. Substituting the stress component σ_{zy} into Equation (1), integrating the resultant expression with respect to y , and ignoring the rigid body displacement, the displacement field becomes

$$w(x, y) = \frac{\delta}{2\pi} \left(\tan^{-1} \left(\tan \frac{\kappa Gy}{2} \coth \frac{\kappa x}{2} \right) - \tan^{-1} \left(\tan \frac{\kappa G(y - 2h_1)}{2} \coth \frac{\kappa x}{2} \right) \right). \quad (21)$$

The stress components (19)–(20) readily satisfy the boundary conditions in Equation (4). Furthermore, choosing the proper branch of the multiple-valued function which is the first term in the right-hand side of Equation (21), it is easy to verify that Equation (6) holds. In the particular case of screw dislocation in the isotropic half-plane, letting $G = 1$ and $h_2 \rightarrow \infty$ in Equations (19)–(21), the displacement and stress fields become

$$w(x, y) = \frac{\delta}{2\pi} \left(\tan^{-1} \left(\frac{y}{x} \right) - \tan^{-1} \left(\frac{y - 2h_1}{x} \right) \right),$$

$$\left\{ \begin{matrix} \sigma_{zx}(x, y) \\ \sigma_{zy}(x, y) \end{matrix} \right\} = \frac{\delta}{2\pi} \mu \left(\frac{1}{(y - 2h_1)^2 + x^2} \left\{ \begin{matrix} y - 2h_1 \\ -x \end{matrix} \right\} - \frac{1}{y^2 + x^2} \left\{ \begin{matrix} y \\ -x \end{matrix} \right\} \right), \quad \text{for } -\infty < y \leq h_1,$$

where μ is the shear modulus of elasticity of the isotropic half-plane. The above solutions are identical to those in [Weertman and Weertman 1992].

To investigate the behavior of stress fields at the dislocation position from Equation (19) we may observe that

$$\tau_{zy}(x, 0) \sim \frac{\delta G G_{zy}}{2\pi x} \quad \text{as } x \rightarrow 0.$$

Note that the above Cauchy-type singularity at the dislocation location is a distinct feature of stress fields in the two-dimensional regions containing a dislocation.

3. Orthotropic strip with multiple cracks and cavities

The dislocation solutions accomplished in Section 2 can be used to analyze strips with multiple cracks and cavities. The cavities are considered as closed-curve cracks without singularity. We consider a strip weakened by M cavities, N_1 embedded cracks, and N_2 edge cracks. Henceforth, we designate cavities, embedded cracks, and edge cracks with the respective subscripts

$$\begin{aligned} i &\in \{1, 2, \dots, M\}, \\ j &\in \{M + 1, M + 2, \dots, M + N_1\}, \\ k &\in \{M + N_1 + 1, M + N_1 + 2, \dots, N\}, \end{aligned}$$

where $N = M + N_1 + N_2$ and represents the total number of defects. The stress components on the local coordinates X_i - Y_i as seen in Figure 1 located on the surface of i -th crack in terms of stress components in x - y coordinates become

$$\sigma_{zY_i} = \sigma_{zy} \cos \varphi_i - \sigma_{zx} \sin \varphi_i, \tag{22}$$

$$\sigma_{zX_i} = \sigma_{zx} \cos \varphi_i + \sigma_{zy} \sin \varphi_i, \tag{23}$$

where φ_i is the angle between X_i and x axes. Suppose dislocations with unknown density B_{zj} are distributed on the infinitesimal segment $d\lambda_j$ located at a point with coordinates (x_j, y_j) on the surface of the j -th crack. The traction on the surface of i -th crack, due to the above distribution of dislocations, and using Equations (19), (20), (22), and (23), becomes

$$\begin{aligned} \sigma_{zY_i}(x_i, y_i) = \frac{G_{zy} B_{zj} d\lambda_j}{4h} &\left(\frac{\cos \varphi_i \sinh \kappa(x_i - x_j) + G \sin \varphi_i \sin \kappa G(y_i - y_j)}{\cosh \kappa(x_i - x_j) - \cos \kappa G(y_i - y_j)} \right. \\ &\left. - \frac{\cos \varphi_i \sinh \kappa(x_i - x_j) + G \sin \varphi_i \sin \kappa G(y_i + y_j - 2h)}{\cosh \kappa(x_i - x_j) - \cos \kappa G(y_i + y_j - 2h)} \right). \end{aligned} \tag{24}$$

Covering crack surfaces by dislocations, the principle of superposition can be invoked to obtain traction on a crack surface. We can thus integrate Equation (24) on the crack surfaces and superimpose the resultant tractions. Integration of Equation (24) is facilitated by describing crack configurations in parametric form $x_i = x_i(s)$, $y_i = y_i(s)$, for $i = 1, 2, \dots, N$, and where $-1 \leq s \leq 1$. The traction on the surface of the i -th crack yields

$$\sigma_{zY_i}(x_i(s), y_i(s)) = \sum_{j=1}^N \int_{-1}^1 b_{zj}(t) k_{ij}(s, t) dt, \tag{25}$$

where $b_{zj}(t)$ is the dislocation density on the nondimensionalized length $-1 \leq t \leq 1$. From Equation (24), the kernel $k_{ij}(s, t)$ is

$$\begin{aligned} k_{ij}(s, t) = \frac{G_{zy} \sqrt{(x'_j(t))^2 + (y'_j(t))^2}}{4h} &\left(\frac{\cos \varphi_i(s) \sinh \kappa(x_i(s) - x_j(t)) + G \sin \varphi_i(s) \sin \kappa G(y_i(s) - y_j(t))}{\cosh \kappa(x_i(s) - x_j(t)) - \cos \kappa G(y_i(s) - y_j(t))} \right. \\ &\left. - \frac{\cos \varphi_i(s) \sinh \kappa(x_i(s) - x_j(t)) + G \sin \varphi_i(s) \sin \kappa G(y_i(s) + y_j(t) - 2h)}{\cosh \kappa(x_i(s) - x_j(t)) - \cos \kappa G(y_i(s) + y_j(t) - 2h)} \right). \end{aligned} \tag{26}$$

Substituting the crack angle $\varphi_i(s) = \tan^{-1}(y'_i(s)/x'_i(s))$ as seen in [Figure 1](#), into [Equation \(26\)](#), the kernel is recast in the more convenient form

$$k_{ij}(s, t) = \frac{G_{zy}}{4h} \sqrt{\frac{(x'_j(t))^2 + (y'_j(t))^2}{(x'_i(s))^2 + (y'_i(s))^2}} \left(\frac{x'_i(s) \sinh \kappa(x_i(s) - x_j(t)) + G y'_i(s) \sin \kappa G(y_i(s) - y_j(t))}{\cosh \kappa(x_i(s) - x_j(t)) - \cos \kappa G(y_i(s) - y_j(t))} - \frac{x'_i(s) \sinh \kappa(x_i(s) - x_j(t)) + G y'_i(s) \sin \kappa G(y_i(s) + y_j(t) - 2h)}{\cosh \kappa(x_i(s) - x_j(t)) - \cos \kappa G(y_i(s) + y_j(t) - 2h)} \right). \quad (27)$$

Making use of [Equation \(27\)](#) we can conclude that $k_{ij}(s, t)$ has Cauchy-type singularity for $i = j$ as $t \rightarrow s$. To illustrate this behavior, applying L'Hopital's rule to [Equation \(27\)](#) gives

$$k_{ii}(s, t) = \frac{a_{-1}}{s - t} + \sum_{m=0}^{\infty} a_m (s - t)^m \quad \text{as } t \rightarrow s,$$

where the coefficient of the singular term $a_{-1} = GG_{zy}/2\pi$. The coefficients $a_m, m = 0, 1, \dots$ are regular functions of variable s in the interval $-1 \leq s \leq 1$ which are too lengthy to be given here. By Bueckner's principle, changing the sign of the left-hand side of [Equation \(25\)](#) gives the traction caused by the external loading on the uncracked strip at the presumed surface of cracks. In [Appendix A](#), we present the Green's function solution of applied traction for a self-equilibrating load on strip edges. Using [Equations \(22\)](#) and [\(A4\)](#), the following traction should be applied on the surface of i -th crack

$$\sigma_{zY_i}(x_i(s), y_i(s)) = \frac{\tau_0}{2Gh} \left(\frac{x'_i(s) \sin \kappa G(y_i(s) - h) + G y'_i(s) \sinh \kappa(x_i(s) - x_0)}{(\cosh \kappa(x_i(s) - x_0) + \cos \kappa G(y_i(s) - h)) \sqrt{(x'_i(s))^2 + (y'_i(s))^2}} - \frac{x'_i(s) \sin \kappa G y_i(s) + G y'_i(s) \sinh \kappa(x_i(s) - x_0)}{(\cosh \kappa(x_i(s) - x_0) + \cos \kappa G y_i(s)) \sqrt{(x'_i(s))^2 + (y'_i(s))^2}} \right).$$

Employing the definition of dislocation density function, the equation for crack opening displacement across the j -th crack is

$$w_j^+(s) - w_j^-(s) = \int_{-1}^s \sqrt{(x'_j(t))^2 + (y'_j(t))^2} b_{zj}(t) dt. \quad (28)$$

The displacement field is single-valued for the surfaces of embedded cracks and cavities. Consequently, the dislocation density functions are subjected to the following closure requirement for $j = 1, 2, \dots, M + N_1$

$$\int_{-1}^1 \sqrt{(x'_j(t))^2 + (y'_j(t))^2} b_{zj}(t) dt = 0. \quad (29)$$

The Cauchy singular integral [Equations \(25\)](#) and [\(29\)](#) are solved simultaneously to determine dislocation density functions. Cavities are defined as closed curved cracks with bounded dislocation density at both ends of the cracks. Thus, for $-1 < t < 1, j = 1, 2, \dots, M$ the dislocation density functions for cavities are expressed as

$$b_{zj}(t) = g_{zj}(t) \sqrt{1 - t^2}. \quad (30)$$

Stress fields for embedded cracks in orthotropic materials are singular at crack tips with square root singularity [Delale 1984]. Thus, the dislocation density functions are represented for $-1 < t < 1$, $j = M + 1, M + 2, \dots, M + N_1$ as

$$b_{zj}(t) = \frac{g_{zj}(t)}{\sqrt{1-t^2}}. \tag{31}$$

For edge cracks, taking the embedded crack tip at $t = -1$, for $-1 < t < 1$, $j = M + N_1 + 1, M + N_1 + 2, \dots, N$ we let

$$b_{zj}(t) = g_{zj}(t) \sqrt{\frac{1-t}{1+t}}. \tag{32}$$

[Liebowitz 1968] gives the stress intensity factors for i -th crack in terms of crack opening displacement as

$$k_{IIILi} = \frac{\sqrt{2}}{4} GG_{zy} \lim_{r_{Li} \rightarrow 0} \frac{w_i^-(s) - w_i^+(s)}{\sqrt{r_{Li}}}, \quad k_{IIIRi} = \frac{\sqrt{2}}{4} GG_{zy} \lim_{r_{Ri} \rightarrow 0} \frac{w_i^-(s) - w_i^+(s)}{\sqrt{r_{Ri}}}, \tag{33}$$

for $j = M + 1, M + 2, \dots, N$, where r is the distance from a crack tip. Setting the points L_i and R_i on the surface of the crack, as shown in Figure 1, yields

$$r_{Li} = \left[(x_i(s) - x_i(-1))^2 + (y_i(s) - y_i(-1))^2 \right]^{\frac{1}{2}}, \quad r_{Ri} = \left[(x_i(s) - x_i(1))^2 + (y_i(s) - y_i(1))^2 \right]^{\frac{1}{2}}. \tag{34}$$

Substituting Equation (31) into Equation (28), deriving the resultant equations, substituting Equation (34) into Equation (33), and finally employing L'Hopital's rule yields the stress intensity factors for embedded cracks

$$k_{IIILi} = \frac{GG_{zy}}{2} \left((x'_i(-1))^2 + (y'_i(-1))^2 \right)^{\frac{1}{4}} g_{zi}(-1), \quad k_{IIIRi} = \frac{-GG_{zy}}{2} \left((x'_i(1))^2 + (y'_i(1))^2 \right)^{\frac{1}{4}} g_{zi}(1),$$

where $i = M + 1, M + 2, \dots, M + N_1$. Analogously, for an edge crack the stress intensity factor is

$$k_{IIILi} = GG_{zy} \left((x'_i(-1))^2 + (y'_i(-1))^2 \right)^{\frac{1}{4}} g_{zi}(-1),$$

where $i = M + N_1 + 1, M + N_1 + 2, \dots, N$.

To calculate hoop stress on the surface of cavities, we employ the definition of dislocation density function valid for $-1 \leq s \leq 1$, $i = 1, 2, \dots, M$

$$\gamma_{zX_i}(x_i(s), y_i(s)) = b_{zi}(s). \tag{35}$$

From Hooke's law and Equation (35), for $-1 \leq s \leq 1$, $i = 1, 2, \dots, M$ the shear stress (see [Lekhnitskii 1963]) becomes

$$\sigma_{zX_i}(x_i(s), y_i(s)) = \frac{G_{zx} G_{zy}}{G_{zx} \sin^2 \varphi_i + G_{zy} \cos^2 \varphi_i} b_{zi}(s). \tag{36}$$

Substituting the crack angle $\varphi_i(s) = \tan^{-1}(y'_i(s)x'_i(s))$ into Equation (36) for $-1 \leq s \leq 1$, $i = 1, 2, \dots, M$ results in

$$\sigma_{zX_i}(x_i(s), y_i(s)) = \frac{G_{zx} \left((x'_i(s))^2 + (y'_i(s))^2 \right)}{(x'_i(s))^2 + G^2 (y'_i(s))^2} b_{zi}(s).$$

We define the nondimensionalized hoop stress for $-1 \leq s \leq 1$, $i = 1, 2, \dots, M$ as

$$\sigma_i(s) = \frac{h\sigma_{zX_i}(x_i(s), y_i(s))}{\tau_0},$$

where h is the strip thickness and τ_0 is the point load applied on the strip.

4. Solution of integral equations

The numerical solution of Equations (25) and (29) is carried out for a strip weakened by cavities, embedded cracks, and edge cracks. The numerical procedure developed by [Erdogan et al. 1973] cannot consider all these defects simultaneously. We have developed a minor generalization of the procedure to provide the needed results. Expanding the continuous functions $g_{zj}(t)$ in Equations (30), (31), and (32), respectively, by Tchebysheff polynomials of first kind $T_l(t)$, second kind $U_l(t)$, and the Jacobi polynomials $P_l^{(1/2, -1/2)}$ for $-1 \leq t \leq 1$ leads to

$$g_{zj}(t) = \begin{cases} \sum_{l=0}^{\infty} B_{jl}U_l(t), & j = 1, 2, \dots, M, \\ \sum_{l=0}^{\infty} B_{jl}T_l(t), & j = M + 1, \dots, M + N_1, \\ \sum_{l=0}^{\infty} B_{jl}P_l(t)^{(1/2, -1/2)}, & j = M + N_1 + 1, \dots, N. \end{cases} \quad (37)$$

Using Equation (37), the integral Equation (25) can be rewritten for $-1 \leq s \leq 1$, $i = 1, 2, \dots, N$ as

$$\begin{aligned} \sigma_{zY_i}(x_i(s), y_i(s)) &= \sum_{j=1}^M \sum_{l=0}^{\infty} B_{jl} \int_{-1}^1 k_{ij}(s, t)U_l(t)\sqrt{1-t^2} dt \\ &+ \sum_{j=M+1}^{M+N_1} \sum_{l=0}^{\infty} B_{jl} \int_{-1}^1 k_{ij}(s, t)\frac{T_l(t)}{\sqrt{1-t^2}} dt + \sum_{j=M+N_1+1}^N \sum_{l=0}^{\infty} B_{jl} \int_{-1}^1 k_{ij}(s, t)P_l(t)^{(1/2, -1/2)}\sqrt{\frac{1-t}{1+t}} dt. \end{aligned} \quad (38)$$

Following [Theocaris and Iokimidis 1977] we conclude that at $s = s_r$, $r = 1, 2, \dots, n - 1$, and $s = 1$ the following approximations hold

$$\int_{-1}^1 k_{ij}(s_r, t)\frac{T_l(t)}{\sqrt{1-t^2}} dt \approx \frac{\pi}{n} \sum_{k=1}^n k_{ij}(s_r, t_k)T_l(t_k), \quad (39)$$

$$\int_{-1}^1 k_{ij}(1, t)\frac{T_l(t)}{\sqrt{1-t^2}} dt \approx n\pi a_{-1}\delta_{ij} + \frac{\pi}{n} \sum_{k=1}^n k_{ij}(1, t_k)T_l(t_k), \quad (40)$$

where δ_{ij} is the Kronecker delta, $s_r = \cos(\pi r/n)$ for $r = 1, 2, \dots, n - 1$, and $t_k = \cos(\pi(2k - 1)/2n)$ for $k = 1, 2, \dots, n$. These are the zeros of $U_{n-1}(s_r)$ and $T_n(t_k)$, respectively. Employing identities for $l \in \mathbb{N}$

$$U_l(t)\sqrt{1-t^2} = \frac{T_l(t) - T_{l+2}(t)}{2\sqrt{1-t^2}}, \quad (41)$$

$$P_l(t)^{(1/2, -1/2)}\sqrt{\frac{1-t}{1+t}} = \frac{\Gamma(l + 1/2)}{\sqrt{\pi}l!} \left(\frac{T_{l-1}(t) + T_l(t) - T_{l+1}(t) - T_{l+2}(t)}{2(1+t)\sqrt{1-t^2}} \right), \quad (42)$$

and Equations (39)–(40), the remaining integrals in Equation (38) can be estimated as

$$\int_{-1}^1 k_{ij}(s_r, t)U_l(t)\sqrt{1-t^2} dt \approx \frac{\pi(1-t_k^2)}{n} \sum_{k=1}^n k_{ij}(s_r, t_k)U_l(t_k), \tag{43}$$

$$\int_{-1}^1 k_{ij}(1, t)U_l(t)\sqrt{1-t^2} dt \approx \frac{\pi(1-t_k^2)}{n} \sum_{k=1}^n k_{ij}(1, t_k)U_l(t_k), \tag{44}$$

$$\int_{-1}^1 k_{ij}(s_r, t)P_l(t)^{(1/2,-1/2)}\sqrt{\frac{1-t}{1+t}} dt \approx \frac{\pi(1-t_k)}{n} \sum_{k=1}^n k_{ij}(s_r, t_k)P_l(t_k)^{(1/2,-1/2)}, \tag{45}$$

$$\int_{-1}^1 k_{ij}(1, t)P_l(t)^{(1/2,-1/2)}\sqrt{\frac{1-t}{1+t}} dt \approx \frac{\pi(1-t_k)}{n} \sum_{k=1}^n k_{ij}(1, t_k)P_l(t_k)^{(1/2,-1/2)}. \tag{46}$$

The integral Equations (29) and (38) at the points $s = s_r, r = 1, 2, \dots, n - 1$ and $s = 1$, by virtue of Equations (41)–(46), can be expressed as

$$\begin{aligned} \sigma_{zY_i}(x_i(s_r), y_i(s_r)) &= \frac{\pi}{n} \sum_{j=1}^M \sum_{k=1}^n (1-t_k^2)k_{ij}(s_r, t_k)g_{zj}(t_k) + \frac{\pi}{n} \sum_{j=M+1}^{M+N_1} \sum_{k=1}^n k_{ij}(s_r, t_k)g_{zj}(t_k) \\ &+ \frac{\pi}{n} \sum_{j=M+N_1+1}^N \sum_{k=1}^n (1-t_k)k_{ij}(s_r, t_k)g_{zj}(t_k), \quad i = 1, \dots, N, \quad r = 1, \dots, n-1, \\ \sigma_{zY_i}(x_i(1), y_i(1)) &= \frac{\pi}{n} \sum_{j=1}^M \sum_{k=1}^n (1-t_k^2)k_{ij}(1, t_k)g_{zj}(t_k) + \frac{\pi}{n} \sum_{j=M+1}^{M+N_1} \sum_{k=1}^n k_{ij}(1, t_k)g_{zj}(t_k) \\ &+ \frac{\pi}{n} \sum_{j=M+N_1+1}^N \sum_{k=1}^n (1-t_k)k_{ij}(1, t_k)g_{zj}(t_k), \quad i = M+N_1+1, \dots, N. \end{aligned}$$

In matrix form the above system of algebraic equations is written

$$\begin{bmatrix} H_{11} & H_{12} & \dots & H_{1N} \\ H_{21} & H_{22} & \dots & H_{2N} \\ \vdots & \vdots & \ddots & \vdots \\ H_{N1} & H_{N2} & \dots & H_{NN} \end{bmatrix} \begin{bmatrix} g_{z1}(t_p) \\ g_{z2}(t_p) \\ \vdots \\ g_{zN}(t_p) \end{bmatrix} = \begin{bmatrix} q_1(s_r) \\ q_2(s_r) \\ \vdots \\ q_N(s_r) \end{bmatrix}. \tag{47}$$

The matrix and vector components in the system of Equation (47) are

$$H_{ij} = \begin{bmatrix} A_{j1}k_{ij}(s_1, t_1) & \dots & A_{j,n-1}k_{ij}(s_1, t_{n-1}) & A_{jn}k_{ij}(s_1, t_n) \\ \vdots & \ddots & \vdots & \vdots \\ A_{j1}k_{ij}(s_{n-1}, t_1) & \dots & A_{j,n-1}k_{ij}(s_{n-1}, t_{n-1}) & A_{jn}k_{ij}(s_{n-1}, t_n) \\ A_{j1}B_{ij}(t_1) & \dots & A_{j,n-1}B_{ij}(t_{n-1}) & A_{jn}B_{ij}(t_n) \end{bmatrix},$$

$$g_{zj} = [g_{zj}(t_1) \dots g_{zj}(t_n)]^T, \quad j = 1, 2, \dots, N,$$

$$q_i = [\sigma_{zY_i}(x_i(s_1), y_i(s_1)) \dots \sigma_{zY_i}(x_i(s_{n-1}), y_i(s_{n-1})) \ 0]^T, \quad i = 1, \dots, M+N_1,$$

$$q_i = [\sigma_{zY_i}(x_i(s_1), y_i(s_1)) \dots \sigma_{zY_i}(x_i(s_{n-1}), y_i(s_{n-1})) \ \sigma_{zY_i}(x_i(1), y_i(1))]^T, \quad i = M+N_1+1, \dots, N.$$

In the above equalities, superscript T stands for the transpose of a vector and A_{jk} and $B_{ij}(t)$ are

$$A_{jk} = \frac{\pi}{n} \begin{cases} 1 - t_k^2, & j = 1, \dots, M, \\ 1, & j = M + 1, \dots, M + N_1, \\ 1 - t_k, & j = M + N_1 + 1, \dots, N, \end{cases} \quad k = 1, 2, \dots, n,$$

$$B_{ij}(t) = \begin{cases} \delta_{ij} \sqrt{(x'_i(t))^2 + (y'_i(t))^2}, & i = 1, \dots, M + N_1, \\ k_{ij}(1, t), & i = M + N_1 + 1, \dots, N. \end{cases}$$

Note that the minor enhancement of [Erdogan et al. 1973] does not affect the convergence of numerical results.

5. Numerical examples and results

The validity of analysis is examined by considering an orthotropic strip with thickness h where the x -axis coincides with the lower edge of strip. The strip is weakened by a single crack located on the y -axis extending over $a \leq y \leq b$. The crack is under antiplane traction $\tau_0(s)$ on its surface. For this example, the integral Equation (25) simplifies to

$$\tau_0(s) = \frac{(b-a)GG_{zy}}{4h} \int_{-1}^1 \frac{\sin(\pi y(t)/h)}{\cos(\pi y(t)/h) - \cos(\pi y(s)/h)} b_z(t) dt, \tag{48}$$

where the crack equation for $-1 \leq s \leq 1$ is

$$y(s) = \frac{1}{2}(b + a + (b - a)s).$$

The integral Equation (48) is identical to Equation (30) derived by [Li 2005]. This may demonstrate that our method is valid for numerical analysis of cracks in strips.

For cavities, the formulations and also the numerical solution of integral equations are validated by considering an infinite isotropic plane weakened by two identical circular approaching cavities. The plane is under uniform antiplane traction τ_0 at infinity. The variation of the nondimensionalized stress component $\sigma_{zy}(d, 0)/\tau_0$ versus the distance between cavities is shown in Figure 2. The results are in reasonable agreement with those obtained by [Steif 1989]. As a final check of the formulation, we

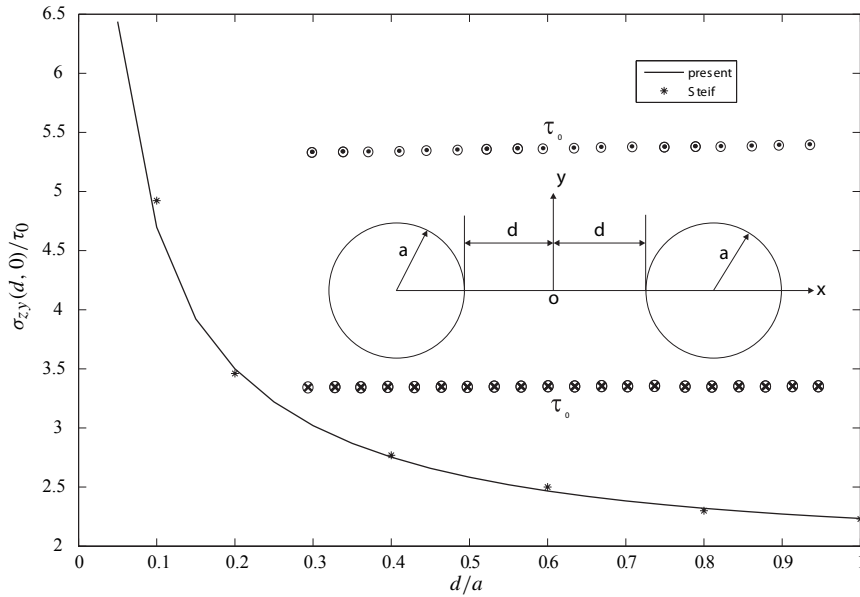


Figure 2. Comparison of hoop stress with Steif's results.

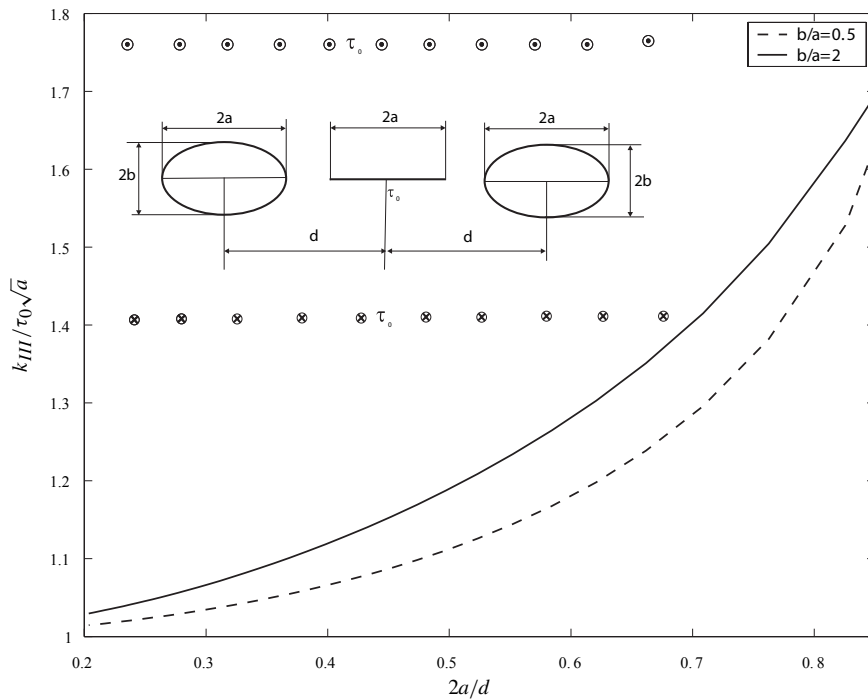


Figure 3. Variation of stress intensity factor with $2a/d$.

analyze an embedded crack located between two approaching elliptical cavities under far field traction (Figure 3), and show that the curves for $k/\tau_0\sqrt{a}$ versus $2a/d$ coincide with Isida's results in [Isida 1973].

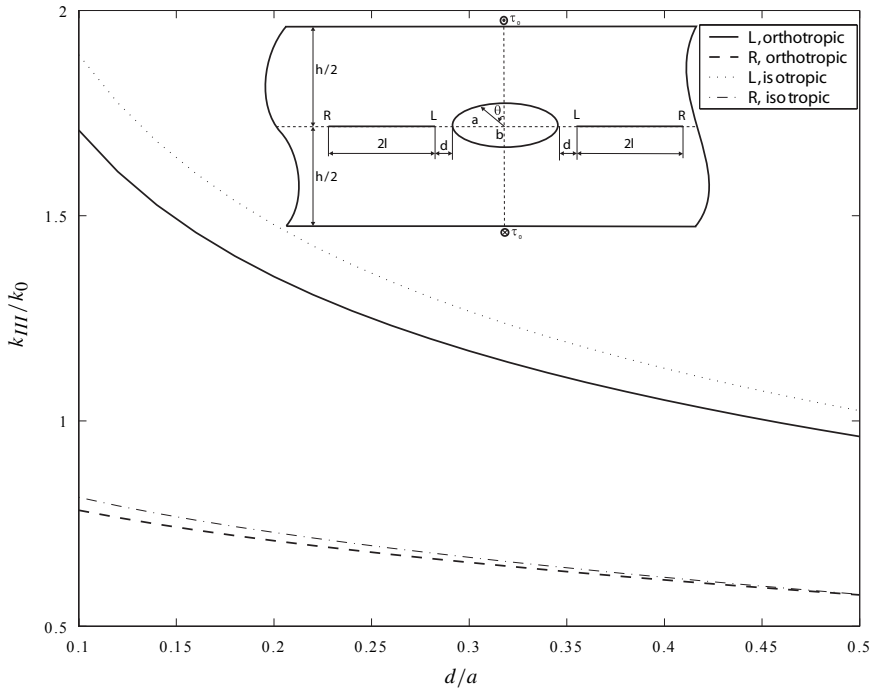


Figure 4. Variations of k_{III}/k_0 with d/a .

The procedure described in the preceding sections allows consideration of a strip with any number of cracks and cavities, and with differing orientations. We now furnish four examples to demonstrate the applicability of this method. In all examples, the ratio of the moduli of elasticity of the orthotropic strip is taken as $G = 1.135$ which is representative of that for carbon-carbon plies. Moreover, the strip is under antiplane point force with magnitude τ_0 on the edges. The stress intensity factors become dimensionless by using the divisor $k_0 = \tau_0 \sqrt{l/h}$, where l is the half length of embedded crack. For an edge crack, l is the crack length.

In the first example, we consider a pair of straight cracks with length $2l = h/3$ and an elliptical cavity with the length of major semi-axis $a = h/6$ and minor semi-axis $b = h/12$. The major axis of the cavity and the cracks are located on the centerline of the strip. Therefore, the problem is symmetric with respect to the y -axis. Figure 4 shows the variations of nondimensionalized stress intensity factors, k/k_0 , of crack tips against d/a for isotropic and orthotropic strips. As the crack tip approaches the elliptical cavity, k/k_0 at the tip L increases rapidly. In the orthotropic strip, weaker material stiffness in the y -direction compared to that of the x -direction reduces the stress intensity factor. The plot of dimensionless hoop stress on the elliptical cavity, $h\sigma_{zX}/\tau_0$, versus angle θ , where θ is measured from the minor-axis of elliptical cavity, are shown for the orthotropic strip in Figure 5. A similar trend for dimensionless hoop stress but with greater magnitude was observed for a cavity in the isotropic strip.

In the second example, we consider an orthotropic strip weakened by an edge crack with length $h/4$ perpendicular to the upper edge of strip, and a rotating embedded crack with length $2l = h/2$. The plots of dimensionless stress intensity factors, k/k_0 , versus the crack orientation, angle θ , are shown in Figure 6. The interaction between cracks is weak, In particular, variation of k/k_0 is small for the edge

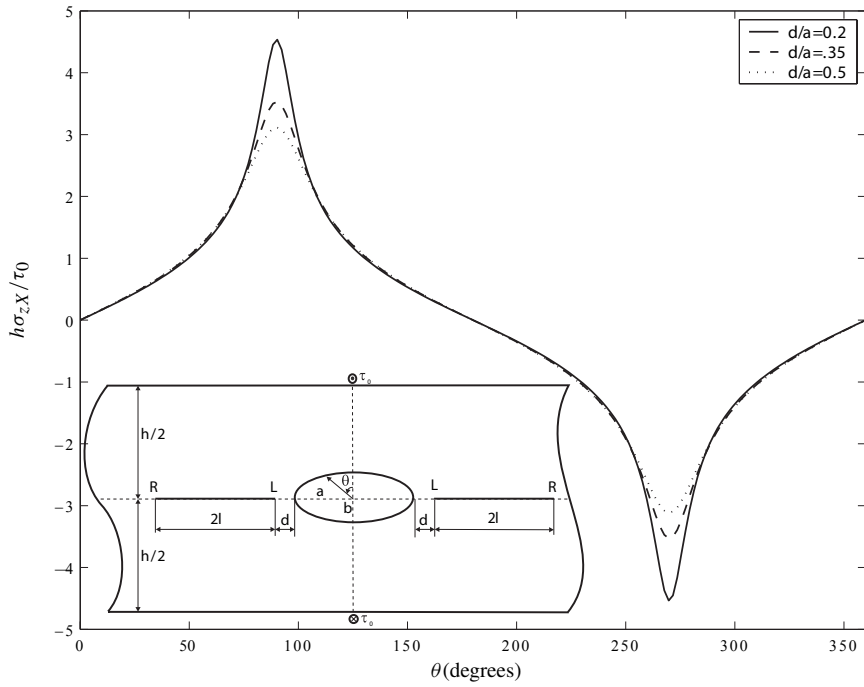


Figure 5. Dimensionless hoop stress on the elliptical cavity for the orthotropic strip versus θ for $d/a = 0.5$.

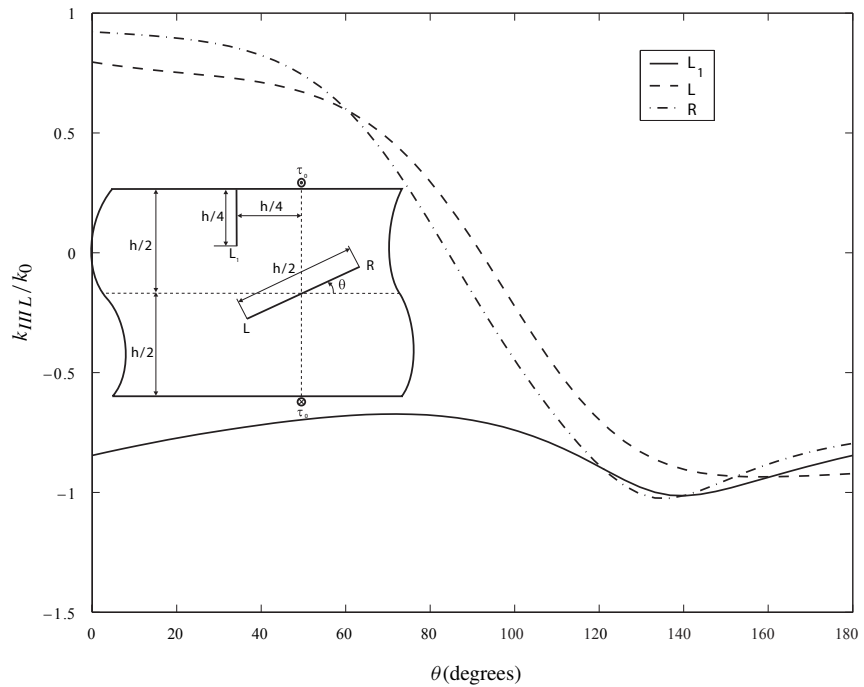


Figure 6. Variations of k_{III}/k_0 with θ for orthotropic strips.

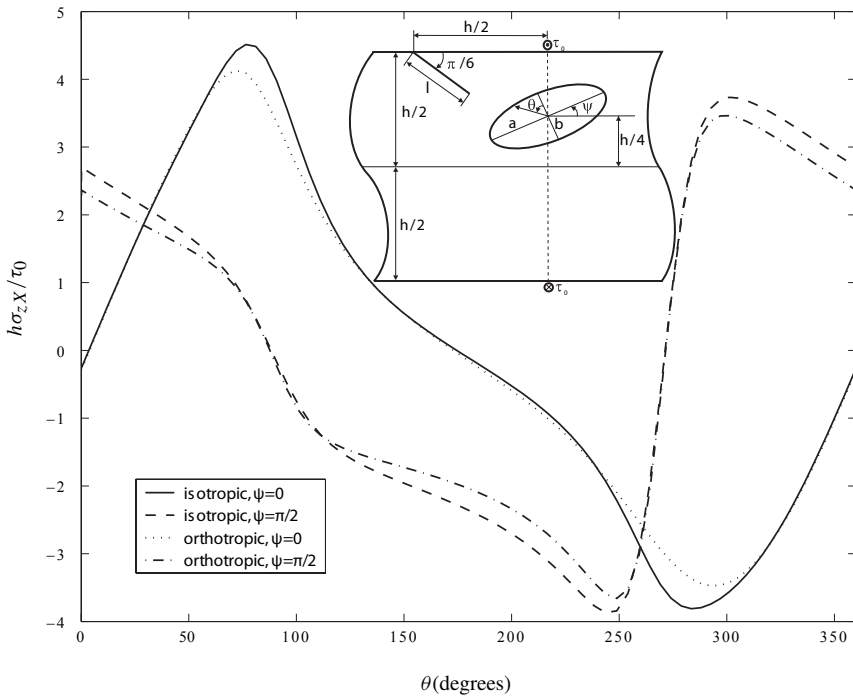


Figure 7. Dimensionless hoop stress on the elliptical cavity versus θ for different values of ψ .

crack. At $\theta = \pi/2$, the embedded crack experiences some stress due to interaction with the edge crack. For the isotropic strip, the plots of k/k_0 are very similar to those in Figure 6, but with slightly reduced magnitude.

In the third example, we consider a strip weakened by a stationary inclined edge crack with length $l = h/3$ and an elliptical cavity with the length of major semi-axis $a = h/8$ and minor semi-axis $b = h/12$. We let the cavity rotate around its center. Figure 7 shows the plot of dimensionless hoop stress for two different orientations of cavity, $\psi = 0$ and $\pi/2$, versus the angle θ , where θ is measured from the minor axis of elliptical cavity. Figure 8 shows dimensionless stress intensity factors, k/k_0 , for the crack tip versus the cavity orientation. For all cavity orientations, the magnitude of the stress intensity factor in the orthotropic strip is higher than that in the isotropic one.

In the fourth and last example, we consider a straight embedded crack with a fixed center, an inclined edge crack, and a circular cavity with radius $R = h/6$. The center of the cavity and the embedded crack are located on the line with distance $h/3$ from the lower edge of strip. The edge crack is in the radial direction of the cavity with a length half of the embedded crack. The distance from the center of the embedded crack to the center of cavity is $4h/3$. Figure 9 and shows the stress intensity factors for edge cracks with changing crack length in isotropic and orthotropic strips, and Figure 10 shows the same information, but for embedded cracks. The dimensionless hoop stress for the cavity, when $l/h = 1$, is shown in Figure 11. Hoop stress is greatest at the points closest to crack tips.

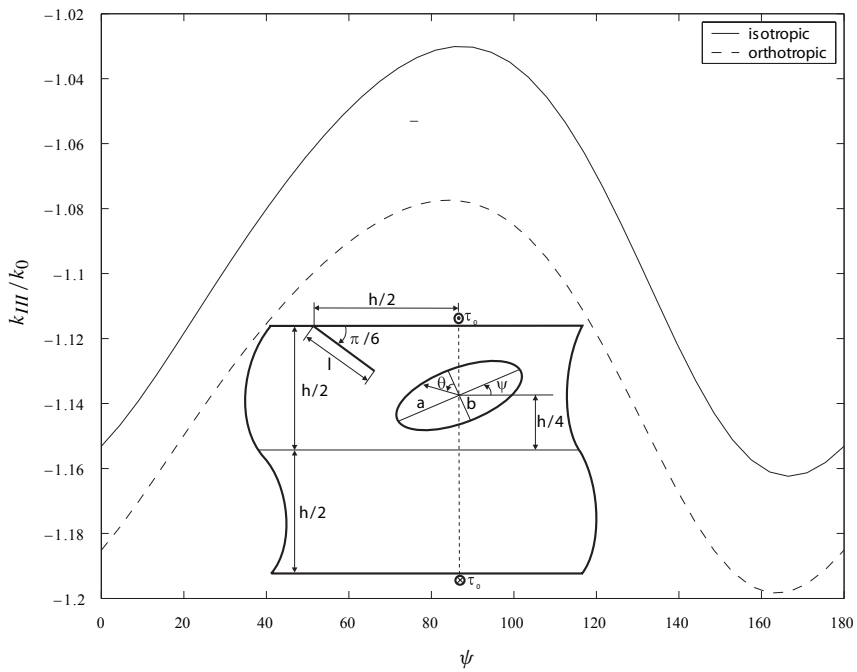


Figure 8. Variations of k_{III}/k_0 with ψ .

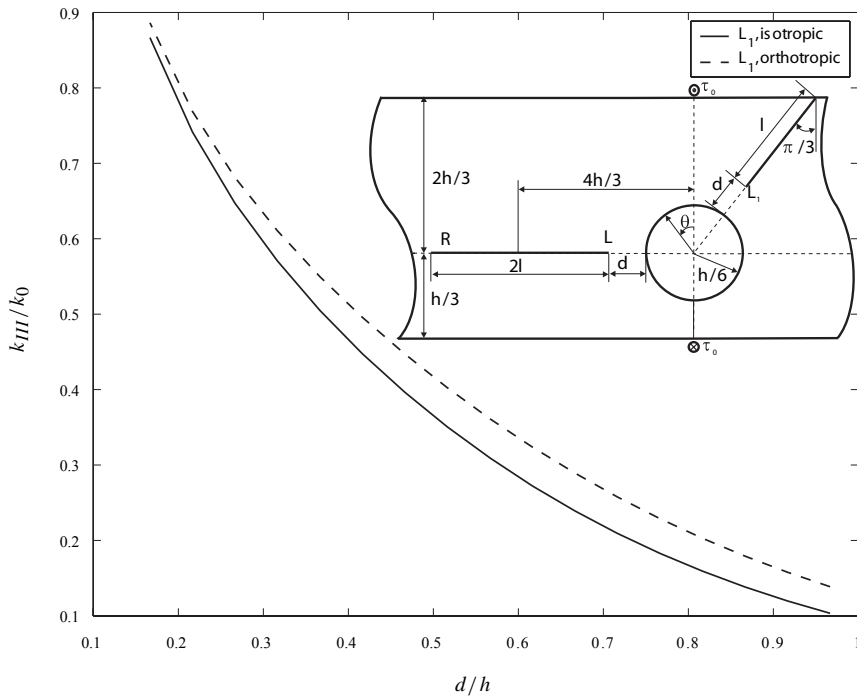


Figure 9. Variations of k_{III}/k_0 with d/h for the edge crack.

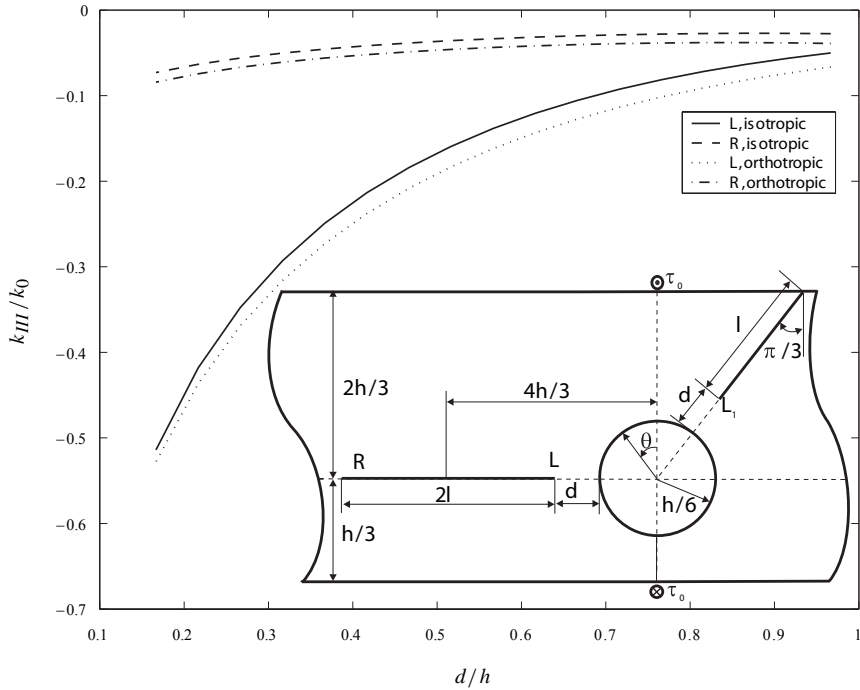


Figure 10. Variations of k_{III}/k_0 with d/h for the embedded crack.

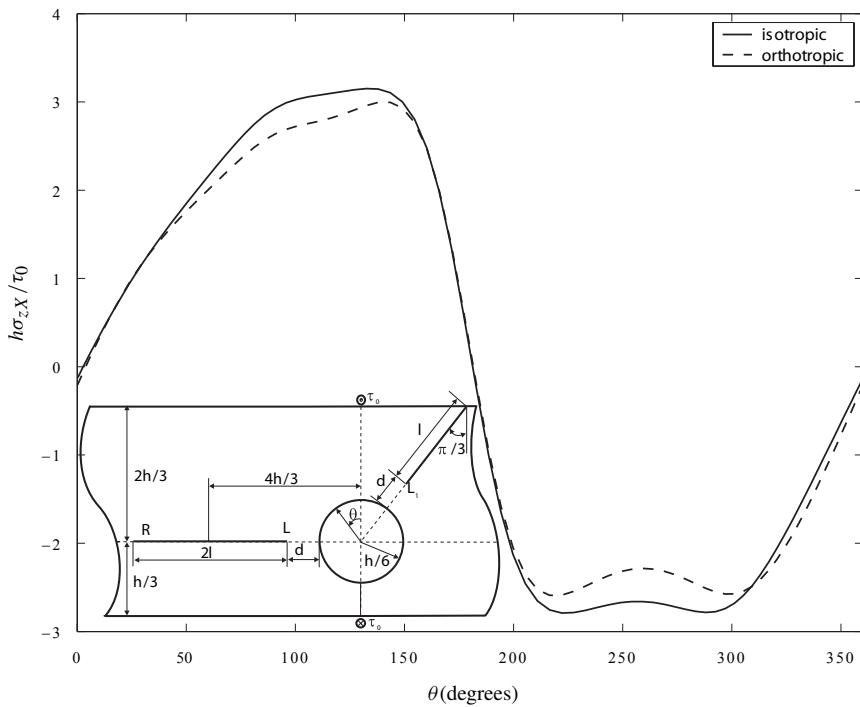


Figure 11. Dimensionless hoop stress on the circular cavity inside the strip versus θ for $l = h$.

Appendix A

The Green's function solution for elasticity problem of a strip under antiplane load may be obtained by applying the following self-equilibrating traction to the strip edges

$$\sigma_{zy}(x, h) = \tau_0 \delta(x - x_0) = \sigma_{zy}(x, 0). \quad (\text{A1})$$

The application of Fourier transform in x -direction to Equation (3) leads to a second order ordinary differential equation with the solution

$$W(\Omega, y) = E(\Omega)e^{\Omega Gy} + F(\Omega)e^{-\Omega Gy}. \quad (\text{A2})$$

The unknown coefficients in Equation (A2) are obtained by taking the Fourier transform of Equation (A1) and applying them to Equation (A2), yielding

$$W(\Omega, y) = \frac{\tau_0}{GG_{zy}} \frac{\cosh \Omega Gy - \cosh \Omega G(y - h)}{\Omega \sinh \Omega Gh} e^{-i\Omega x_0}. \quad (\text{A3})$$

Employing the inverse Fourier transform of Equation (A3) in conjunction with Equations (1)–(2) give the stress fields as

$$\sigma_{zx}(x, y) = \frac{i\tau_0 G}{2\pi} \int_{-\infty}^{\infty} \frac{\cosh \Omega Gy - \cosh \Omega G(y - h)}{\sinh \Omega Gh} e^{i\Omega(x-x_0)} d\Omega,$$

$$\sigma_{zy}(x, y) = \frac{\tau_0}{2\pi} \int_{-\infty}^{\infty} \frac{\sinh \Omega Gy - \sinh \Omega G(y - h)}{\sinh \Omega Gh} e^{i\Omega(x-x_0)} d\Omega.$$

To determine the above integrals, we can use contour integration. The results are

$$\sigma_{zx}(x, y) = \frac{\tau_0}{2h} \left(\frac{\sinh \kappa(x - x_0)}{\cosh \kappa(x - x_0) + \cos \kappa G(y - h)} - \frac{\sinh \kappa(x - x_0)}{\cosh \kappa(x - x_0) + \cos(\kappa Gy)} \right), \quad (\text{A4})$$

$$\sigma_{zy}(x, y) = \frac{\tau_0}{2Gh} \left(\frac{\sin \kappa Gy}{\cosh \kappa(x - x_0) + \cos \kappa Gy} - \frac{\sin \kappa G(y - h)}{\cosh \kappa(x - x_0) + \cos \kappa G(y - h)} \right). \quad (\text{A5})$$

References

- [Delale 1984] F. Delale, "Stress singularities in bonded anisotropic materials", *Int. J. Solids Struct.* **20**:1 (1984), 31–40.
- [Erdogan et al. 1973] F. Erdogan, G. D. Gupta, and T. S. Cook, "Numerical solution of integral equations", pp. 368–425 in *Methods of analysis and solutions of crack problems*, edited by G. C. Sih, Mechanics of Fracture **1**, Noordhoff, Leyden, 1973.
- [Isida 1973] M. Isida, "Method of Laurent series expansion for internal crack problems", pp. 56–130 in *Methods of analysis and solutions of crack problems*, edited by G. C. Sih, Mechanics of Fracture **1**, Noordhoff, Leyden, 1973.
- [Lekhnitskii 1963] S. G. Lekhnitskii, *Theory of elasticity of an anisotropic elastic body*, Holden-Day, San Francisco, 1963.
- [Li 2003] X. F. Li, "Closed-form solution for two collinear mode-III cracks in an orthotropic elastic strip of finite width", *Mech. Res. Commun.* **30**:4 (2003), 365–370.
- [Li 2005] X. F. Li, "Two perfectly-bonded dissimilar orthotropic strips with an interfacial orthotropic strips normal to the boundaries", *Appl. Math. Comp.* **163**:2 (2005), 961–975.
- [Liebowitz 1968] H. Liebowitz, *Fracture mechanics*, Academic Press, New York, 1968.
- [Steif 1989] P. S. Steif, "Stress concentration around a pair of circular holes", *J. Appl. Mech. (ASME)* **56** (1989), 719–721.

- [Theocaris and Iokimidis 1977] P. S. Theocaris and N. I. Iokimidis, “Numerical integration methods for the solution of singular integral equations”, *Q. Appl. Math.* **35** (1977), 173–183.
- [Weertman and Weertman 1992] J. Weertman and J. R. Weertman, *Elementary dislocation theory*, Oxford University Press, New York, 1992.
- [Wu and Dzenis 2002] X. F. Wu and Y. A. Dzenis, “Closed-form solution for a mode-III interfacial edge crack between two bonded dissimilar elastic strips”, *Mech. Res. Commun.* **29**:5 (2002), 407–412.
- [Zhou and Ma 1999] Z. G. Zhou and L. Ma, “Two collinear Griffith cracks subjected to anti-plane shear in infinitely long strip”, *Mech. Res. Commun.* **26**:4 (1999), 437–444.
- [Zhou et al. 1998] Z. G. Zhou, B. Wang, and S. Y. Du, “The stress field in the vicinity of two collinear cracks subject to antiplane shear in a strip of finite width”, *Mech. Res. Commun.* **25**:2 (1998), 183–188.

Received 11 Dec 2005. Revised 18 Feb 2006. Accepted 24 May 2006.

REZA TEYMORI FAAL: faal92@yahoo.com

Department of Mechanical Engineering, Amirkabir University of Technology (Tehran Polytechnic), 424 Hafez Avenue, Tehran 158754413, Iran

SHAHRIAR J. FARIBORZ: sjfariborz@yahoo.com

Department of Mechanical Engineering, Amirkabir University of Technology (Tehran Polytechnic), 424 Hafez Avenue, Tehran 158754413, Iran

HAMID REZA DAGHYANI: Deceased 2006

Department of Mechanical Engineering, Amirkabir University of Technology (Tehran Polytechnic), 424 Hafez Avenue, Tehran 158754413, Iran